Evidence for the Isoscalar Giant Dipole Resonance in ^{208}Pb Using Inelastic α Scattering at and near 0°

B. F. Davis,[1] U. Garg,[1] W. Reviol,[1,*] M. N. Harakeh,[2] A. Bacher,[3] G. P. A. Berg,[3] C. C. Foster,[3] E. J. Stephenson,[3]
Y. Wang,[3] J. Jänecke,[4] K. Pham,[4] D. Roberts,[4] H. Akimune,[5] M. Fujiwara,[5] and J. Lisantti[6]
[1]*Department of Physics, University of Notre Dame, Notre Dame, Indiana 46556*
[2]*KVI, 9747 AA Groningen, The Netherlands*
[3]*Indiana University Cyclotron Facility, 2401 Milo B. Sampson Lane, Bloomington, Indiana 47405*
[4]*Department of Physics, University of Michigan, Ann Arbor, Michigan 48109*
[5]*Research Center for Nuclear Physics, Osaka University, Mihogaoka 10-1, 567 Osaka, Japan*
[6]*Department of Physics, Centenary College, Shreveport, Louisiana 71134*

(Received 14 November 1996)

The isoscalar giant dipole resonance (ISGDR) in ^{208}Pb has been investigated using inelastic scattering of 200 MeV α particles at and near 0° where the angular distribution of the ISGDR can be clearly differentiated from those of other modes. The "difference of spectra" technique was employed to separate the ISGDR from the high-energy octupole resonance (HEOR). These data provide the clearest evidence yet for the ISGDR adjacent to the HEOR. With these results, all expected isoscalar $\lambda \leq 3$ resonances in ^{208}Pb have been identified. [S0031-9007(97)03674-0]

PACS numbers: 24.30.Cz, 24.10.Eq, 25.55.Ci, 27.80.+w

Among the low-λ giant resonance modes, the isoscalar dipole resonance (ISGDR) has remained the most intriguing and least investigated. Indeed, most compilations of the giant resonance modes routinely leave the space for the $\Delta T = 0$, $\Delta L = 1$ vibration blank [1] because, to first order, this mode would correspond to only the center-of-mass motion. This Letter reports our investigation of the ISGDR. An "exotic" mode of collective vibration, it is best described as a "hydrodynamical density oscillation" in which the volume of the nucleus remains constant and the state can be visualized in the form of a compression wave—analogous to a sound wave—oscillating back and forth through the nucleus; this phenomenon also has been referred to as the "squeezing mode" [2,3]. This is a second-order effect; as mentioned earlier, in the first order, the isoscalar dipole mode corresponds to a spurious center-of-mass motion.

In addition to being of substantial intrinsic interest as an exotic and fundamental mode of collective oscillation, the ISGDR also is important in that it can provide, like the giant monopole resonance (GMR), a direct measurement of the nuclear incompressibility. The excitation energy of the ISGDR is given by the scaling model [4] as

$$E_{\mathrm{ISGDR}} = \hbar \sqrt{\frac{7}{3} \frac{K_A + \frac{27}{25}\epsilon_F}{m\langle r^2 \rangle}}\,, \qquad (1)$$

where K_A is the incompressibility of the nucleus and ϵ_F is the Fermi energy. The most common, and well-known, experimental determination of the nuclear incompressibility, so far, has been achieved via measurement of the excitation energies of the GMR, the systematics of which are quite well established [1]. There have been concerns, however, about the suitability of the available GMR data alone in the extraction of the nuclear incompressibility of infinite nuclear matter (see, for example, Refs. [5–7]). A detailed and systematic investigation of the ISGDR could provide additional information, leading, it is hoped, to a more precise determination of the incompressibility of nuclear matter.

The evidence for the ISGDR has been rather sparse so far. Indications for this resonance have been reported in inelastic scattering experiments at forward angles on ^{208}Pb and ^{144}Sm [8–11]. Since it lies very close in energy to the high-energy octupole resonance (HEOR), an unambiguous identification of the ISGDR is possible only at angles near 0°. This is based on distorted-wave Born approximation (DWBA) calculations (shown in Fig. 1) which indicate that appreciable differences in the angular

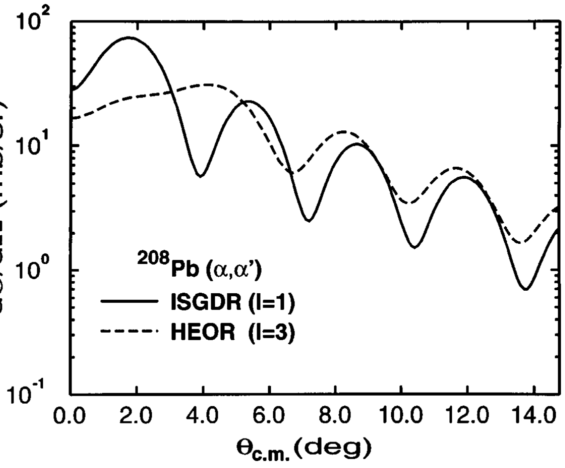

FIG. 1. Differential cross sections for the ISGDR (solid line) and the HEOR (dashed line) assuming 100% exhaustion of the respective energy-weighted-sum-rules (EWSR), as obtained in a DWBA calculation using the program CHUCK3.

© 1997 The American Physical Society

distributions of the two resonances appear only in the near-0° (≤5°) angular region. The situation, thus, is quite similar to that of the GMR almost two decades ago: unambiguous evidence for the GMR could be established only by measurements at the smallest angles where the GMR angular distribution differs substantially from that of the giant quadrupole resonance (GQR) which lies at an excitation energy very close to that of the GMR.

Figure 1 shows the inelastic α-scattering angular distributions for the ISGDR and HEOR in ^{208}Pb over the angular range 0°–14°, calculated in DWBA with the program CHUCK3 [12]. The optical-model parameters used in this calculation were $V = 155$ MeV, $r = 1.282$ fm, $a = 0.677$ fm, $W = 23.26$ MeV, $r_w = 1.478$ fm, $a_w = 0.733$ fm, and $r_C = 1.3$ fm and were adopted from Ref. [13]. For the HEOR, the standard collective form factor [14] was used; for the ISGDR, the form factor was taken from Ref. [3] which also includes the relevant sum-rule expressions and related details. Inelastic scattering of α particles near 0° has the advantage that, because of the isoscalar nature of this reaction, only these two giant resonances are expected to be predominantly excited at the excitation energies of interest. In addition, as indicated by the calculations presented in Fig. 1, the cross sections for these resonances are at or near their maximum values at these angles.

In this Letter, we report the first results of a detailed investigation of the ISGDR in ^{208}Pb to obtain conclusive evidence for this resonance via measurements at very small angles. While the ultimate proof for the ISGDR would, arguably, come from measurement of a complete angular distribution over the range 0°–5°, the expected angular distributions for the HEOR and the ISGDR, nonetheless, allow for the identification of the ISGDR via the "difference of spectra" technique, a procedure used with significant success in detailed investigations of the GMR [15]. Briefly, the inelastic spectrum near 0° (0° → 2° in case of our measurement) may be divided into two parts (0° → 1° and 1° → 2°, respectively). Since the ISGDR cross section rises rapidly in this angular region, whereas the HEOR cross section remains nearly constant (see Fig. 1), if the spectrum from the (0° → 1°) angular cut is subtracted from that for the (1° → 2°) cut, the difference of these two spectra would show only a small contribution from the HEOR, or the background. In principle, this "subtracted spectrum" would yield a rather accurate representation of primarily the ISGDR strength.

Our measurements were performed at the Indiana University Cyclotron Facility and employed a 200 MeV α beam incident on an enriched 3.0 mg/cm^2 thick ^{208}Pb target. Inelastically scattered α particles were detected in the focal plane of the K600 High Resolution Spectrometer operating in the transmission (0°) mode [16]. The usable excitation-energy bite in this mode was 14–29 MeV, appropriate for the aforementioned resonances which are expected to lie at excitation energies of 20–22 MeV in ^{208}Pb. A ^{24}Mg target was used to provide the energy calibration. The energy resolution achieved in these measurements was ~130 keV, more than sufficient to investigate these broad resonances in the singles mode.

Inelastic scattering measurements at small angles, as is well known, require a very careful tuning of the beam to minimize the contributions to the spectra from beam-halo and slit scattering, etc. After considerable effort, it was possible to obtain a rather "clean" beam whereby for 2 nA (electrical) of beam current, the blank target (empty target frame) runs yielded a count rate of about 190 counts/sec (spread almost evenly over the entire spectrum and without any enhancement in the giant resonance region) as compared to an event rate of about 580 counts/sec with the target in place.

The K600 detector system consisted of two sets of x and y position-sensitive wire chambers separated by 10.5 cm in order to allow angle measurements; our ray-tracing technique yielded an angular resolution of 2.1 and 3.0 mrad in the vertical and horizontal directions, respectively. Two scintillation detectors were mounted behind the wire chambers. They provided particle identification and gave fast timing signals for the time-of-flight spectra relative to the phase-compensated cyclotron rf. All information from these detectors was used in the off-line analyses to reduce the background as much as possible. For example, significant "cleaning" of the spectra could be achieved by gating on the TOF signal from the scintillators and, thus, eliminating contributions from scattering occurring "upstream" from the target.

Figure 2(a) shows the 0° → 2° inelastic scattering spectrum for ^{208}Pb. A broad "bump," most likely comprised of the ISGDR and the HEOR, is clearly visible above the background. The data have been fitted with a polynomial background and two Gaussian peaks, and the results of the fit are shown superimposed; using a single, wider peak always resulted in a significantly worse fit. The centroids of the two peaks (19.7 ± 0.5 MeV and 22.4 ± 0.5 MeV) agree with the energies previously suggested [8–10] for the HEOR and ISGDR, respectively. The "difference" spectrum, obtained by subtracting the (0° → 1°) cut from the (1° → 2°) cut, as described previously, is shown in Fig. 2(b) along with a fit employing peak parameters identical to those used in the peak fits shown in Fig. 2(a). In this case, an unconstrained fit always preferred a single, slightly broader, peak; the fit as shown was obtained by deliberately requiring a two-peak fit to the data in order to show the reduction in the strength of one of the components. The rise in the "background" at energies above 25 MeV, visible especially in the subtracted spectrum, is "instrumental": the data close to 2° have contribution from scattering off a metal piece near the end of the detector.

As can be seen, the "HEOR component" of the bump is completely eliminated in this spectrum, leaving only the "ISGDR component," as expected from the angular

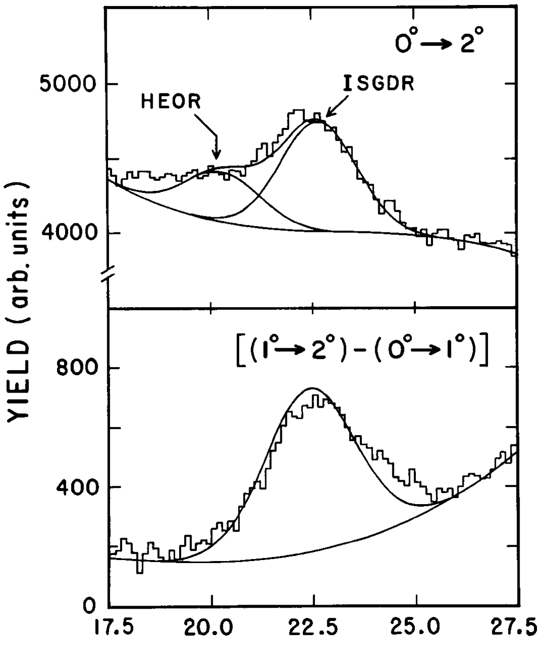

FIG. 2. (a) Inelastic α-scattering spectra for ^{208}Pb for (0 ± 2)°. A two-peak + polynomial-background fit to the data is shown superimposed with the peaks corresponding to the HEOR and the ISGDR indicated. (b) The "difference" spectrum, obtained as described in the text. Also shown is a fit using peak parameters identical to those in (a) note that the fit corresponds to no HEOR strength.

distributions shown in Fig. 1. Our results for the ISGDR are presented in Table I and compared with previous measurements as well as the theoretical predictions for this resonance. Although our results for the centroid energies of the ISGDR and HEOR are in agreement with previous measurements, the widths differ considerably. The reason for the larger widths observed in the earlier measurements is not very clear, but may have to do with the fact that in none of those measurements were the peaks clearly seen, and in the proton scattering measurements, contributions from Coulomb excitation of the IVGQR may have compromised the results. We note, however, that the position and width of the ISGDR extracted from our data are in very good agreement with the theoretical predictions for this resonance by Murav'ev and Urin [18] and van Giai and Sagawa [20].

TABLE I. Parameters of ISGDR in ^{208}Pb.

	E_x (MeV)	Γ (MeV)
200 MeV (α, α') [This work]	22.4 ± 0.5	3.0 ± 0.5
172 MeV $(\alpha, \alpha')^{a}$	21.3 ± 0.8	5.9 ± 0.8
340 and 480 MeV $(\alpha, \alpha')^{b}$	26–35	...
201 MeV $(p, p')^{c}$	21.5 ± 0.2	5.7 ± 0.2
800 MeV $(p, p')^{d}$	22.6 ± 0.2	6.1 ± 0.2
Theory: Murav'ev and Urin[e]	21.4	3.8
Theory: de Haro *et al.*[f]	23	3.5
Theory: Sagawa and van Giai [SGII][g]	22.5[h]	3.2
Theory: Decharge and Gogny[i]	26	...

[a] Reference [8]. [b] Reference [17]. [c] Reference [10].
[d] Reference [11]. [e] Reference [18]. [f] Reference [19].
[g] Reference [20]. [h] Centroid energy. [i] As quoted in Ref. [17].

The above conclusion regarding the ISGDR draws additional support from a comparison of the centroids of the total GR bumps (including both the peaks identified above) in the two spectra: the centroid of the difference spectrum (22.4 MeV) is located more than 1 MeV higher in excitation energy than that in the full spectrum (21.3 MeV), again consistent with a reduction in the HEOR strength as expected from the calculated angular distributions for the HEOR and the ISGDR. The bump in Fig. 2(b), thus, corresponds primarily to the ISGDR strength and can be subjected to further investigation to extract the properties of this resonance.

Further extension of this analysis has been possible by dividing the data into 0.5°-wide angular bins, corresponding to 0° → 0.5°, 0.5° → 1.0°, 1.0° → 1.5°, and 1.5° → 2.0°, thus providing a limited angular distribution for the two components of the GR bump identified above as the HEOR and ISGDR. Figure 3 shows three of these spectra along with results of simultaneous, multispectrum, two-peak fits to the data (fits to the 1.5° → 2° part were deemed unreliable because of the instrumental contribution to the background mentioned above).

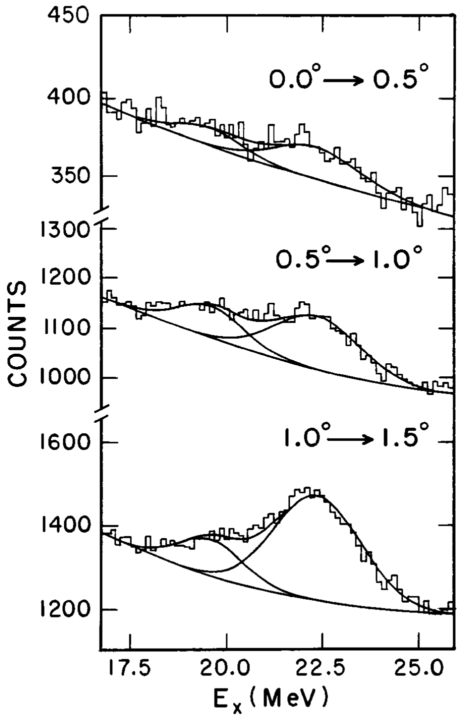

FIG. 3. Inelastic α scattering spectra for ^{208}Pb for the angle bins indicated. Two-peak + polynomial-background fits to the data are shown superimposed.

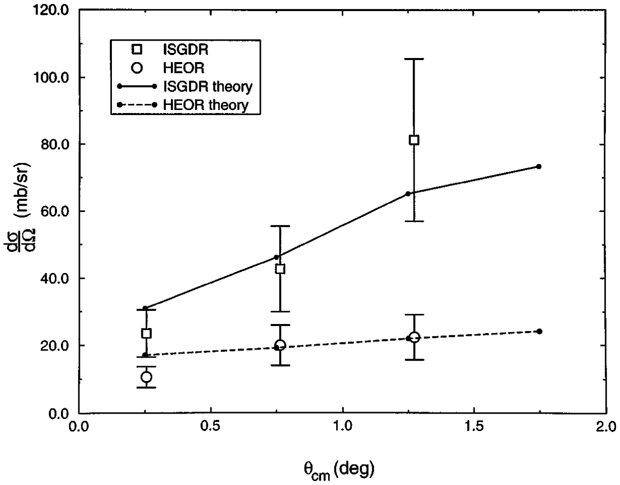

FIG. 4. "Angular distributions" for the two components of the GR bump. The open circles and squares, respectively, represent peak 1 and peak 2 described in the text; the errors shown are lower-bound estimates. The solid and dashed lines connect the theoretical cross sections (corresponding to 100% EWSR) for the ISGDR and HEOR, respectively, obtained from DWBA calculations and averaged over the 0.5° width of the angular bins.

Figure 4 shows these "angular distributions" for the two components and compares them with the angular distributions for the ISGDR and HEOR expected from DWBA calculations based on 100% of the respective EWSR. The experimental data appear to follow the qualitative behavior of the expected angular distributions quite well. Considering the rather limited statistics in the spectra associated with individual angular bins and the uncertainties in the angular cuts, this agreement is, indeed, remarkable. The observed strength exhausts the full EWSR for both resonances, in agreement (within the uncertainties) with ~70% and ~85% expected for the HEOR and ISGDR, respectively, based on earlier measurements of the low-lying isoscalar octupole and dipole strengths in ^{208}Pb [21,22].

Using the excitation energy of the ISGDR obtained from this experiment, Eq. (1) gives a value for the nuclear incompressibility K_A for ^{208}Pb to be 126 ± 6 MeV. This is about 13% lower than the value (145 MeV) obtained from the energy of the isoscalar monopole resonance in this nucleus [23]. Systematics of the ISGDR are therefore urgently needed to establish whether this is a genuine effect, or merely indicative of the fact that some of the ISGDR strength in ^{208}Pb is spread to higher excitation energies as suggested, for example, by some theoretical calculations [20].

In conclusion, we have measured inelastic α-scattering spectra at and near 0° and used the difference of spectra technique to obtain the clearest evidence so far for the ISGDR, located adjacent to the HEOR in ^{208}Pb. The extracted excitation energies of these two resonances are in agreement with those previously suggested for ISGDR and HEOR in ^{208}Pb, as well as with recent theoretical calculations. With the present result, all the expected isoscalar $\lambda \leq 3$ resonances have been identified for ^{208}Pb.

We acknowledge the cooperation of the operations crew of the Indiana University Cyclotron Facility in providing high-quality α beams for these measurements. This work has been supported in part by the U.S. National Science Foundation and the NATO Division of Scientific Affairs.

---

*Present address: Department of Physics and Astronomy, University of Tennessee, Knoxville, TN 37996.

[1] See, for example, A. van der Woude, in *Electric and Magnetic Giant Resonances in Nuclei,* edited by J. Speth (World Scientific, Singapore, 1991), p. 100.
[2] M. N. Harakeh, Phys. Lett. **90B**, 13 (1980).
[3] M. N. Harakeh and A. E. L. Dieperink, Phys. Rev. C **23**, 2329 (1981).
[4] S. Stringari, Phys. Lett. **108B**, 232 (1982).
[5] J. M. Pearson, Phys. Lett. B **271**, 12 (1991).
[6] M. M. Sharma, in Slide Report for the Notre Dame Workshop on Giant Resonances and Related Phenomena, Notre Dame, 1991, edited by U. Garg (unpublished).
[7] S. Shlomo and D. H. Youngblood, Phys. Rev. C **47**, 529 (1993); Nucl. Phys. **A569**, 303c (1994).
[8] H. P. Morsch *et al.*, Phys. Rev. Lett. **45**, 337 (1980).
[9] H. P. Morsch *et al.*, Phys. Rev. C **28**, 1947 (1983).
[10] C. Djalali *et al.*, Nucl. Phys. **A380**, 42 (1982).
[11] G. S. Adams *et al.*, Phys. Rev. C **33**, 2054 (1986).
[12] P. D. Kunz, University of Colorado, 1983 (unpublished).
[13] D. A. Goldberg *et al.*, Phys. Rev. C **7**, 1938 (1973).
[14] G. R. Satchler, Part. Nuclei **5**, 105 (1973).
[15] S. Brandenburg *et al.*, Nucl. Phys. **A446**, 29 (1987).
[16] G. P. A. Berg *et al.*, IUCF Scientific and Technical Report, 1990–1991, p. 221 (unpublished).
[17] B. Bonin *et al.*, Nucl. Phys. **A430**, 349 (1984).
[18] S. E. Murav'ev and M. G. Urin, Bull. Acad. Sci. USSR (Phys. Ser.) **52**, 123 (1988).
[19] R. de Haro, S. Krewald, and J. Speth, Phys. Rev. C **26**, 1649 (1982).
[20] N. van Giai and H. Sagawa, Nucl. Phys. **A371**, 1 (1981).
[21] M. N. Harakeh *et al.*, Nucl. Phys. **A327**, 373 (1979).
[22] T. D. Poelhekken *et al.*, Phys. Lett. B **278**, 12 (1992).
[23] D. H. Youngblood *et al.*, Phys. Rev. C **23**, 1997 (1981).